Extremophiles (2005) 9:449–460
DOI 10.1007/s00792-005-0462-3

ORIGINAL PAPER

Sumihiro Koyama · Hiromi Kobayashi · Akira Inoue
Tetsuya Miwa · Masuo Aizawa

Effects of the piezo-tolerance of cultured deep-sea eel cells on survival rates, cell proliferation, and cytoskeletal structures

Received: 14 March 2005 / Accepted: 30 May 2005 / Published online: 5 August 2005

Abstract We investigated the pressure tolerance of deep-sea eel (*Simenchelys parasiticus*; habitat depth, 366–2,630 m) cells, conger eel (*Conger myriaster*) cells, and mouse 3T3-L1 cells. Although there were no living mouse 3T3-L1 and conger eel cells after 130 MPa (0.1 MPa = 1 bar) hydrostatic pressurization for 20 min, all deep-sea eel cells remained alive after being subjected to pressures up to 150 MPa for 20 min. Pressurization at 40 MPa for 20 min induced disruption of actin and tubulin filaments with profound cell-shape changes in the mouse and conger eel cells. In the deep-sea eel cells, microtubules and some actin filaments were disrupted after being subjected to hydrostatic pressure of 100 MPa and greater for 20 min. Conger eel cells were sensitive to pressure and did not grow at 10 MPa. Mouse 3T3-L1 cells grew faster under pressure of 5 MPa than at atmospheric pressure and stopped growing at 18 MPa. Deep-sea eel cells were capable of growth in pressures up to 25 MPa and stopped growing at 30 MPa. Deep-sea eel cells required 4 h at 20 MPa to finish the M phase, which was approximately fourfold the time required under atmospheric conditions.

Keywords Piezo-tolerance · Deep-sea fish cells · Actin · Tubulin · Depolymerization · Hydrostatic pressure

Communicated by K. Horikoshi

S. Koyama (✉) · T. Miwa
Extremobiosphere Research Center,
Japan Agency for Marine-Earth Science and Technology,
2-15 Natsushima-cho, Yokosuka 237-0061, Japan
E-mail: skoyama@jamstec.go.jp
Tel.: +81-468-679691
Fax: +81-468-679715

H. Kobayashi
Department of Biological Information,
Graduate School of Bioscience and Biotechnology,
Tokyo Institute of Technology, Nagatsuta,
Yokohama 226-8501, Japan

A. Inoue
Faculty of Life Sciences, Toyo University, 1-1-1 Izumino,
Itakura-machi, Ora-gun, Gunma 374-0193, Japan

M. Aizawa
Tokyo Institute of Technology, O-okayama, Meguro-ku,
Tokyo 152-8550, Japan

Introduction

Since the establishment of a variety of mammalian cell lines, great interest has been focused on the molecular and cellular biological properties of mammals. Although recent increasing attention has been paid to deep-sea multicellular organisms, no cell line from such organisms has been successfully established. The culture of tissues derived from deep-sea multicellular organisms has been difficult because of the damage they sustain upon decompression and exposure to the high temperatures of surface seawater. Even if deep-sea creatures can be maintained alive for short periods, contamination by microorganisms hinders their primary culture (Koyama and Aizawa 2000). Therefore, it has been extremely difficult to study the molecular and cellular biological properties of deep-sea organisms.

In our recent study, we have developed a novel piezostat aquarium system to capture and maintain deep-sea multicellular organisms (Koyama et al. 2002a). Using this system, we have succeeded in maintaining a variety of deep-sea multicellular organisms under pressure (Koyama et al. 2002a, 2003a, 2003b, 2005) and under atmospheric conditions after gradual, slow decompression (Koyama et al. 2003a, 2003b, 2005).

In our recent study, the deep-sea eel *Simenchelys parasiticus* (habitat depth, 366–2,630 m; Nakabo 2000) captured from an ocean depth of 1,162 m survived under atmospheric pressure for 5 days after gradual, slow decompression (Koyama et al. 2003a, 2003b). Using the living deep-sea eel *S. parasiticus*, we successfully cultivated pectoral fin cells in salt-enriched L-15 medium supplemented with fetal bovine serum (FBS) at

atmospheric pressure (Koyama et al. 2003a, 2003b). We confirmed that the deep-sea eel cells passaged more than 20 times and succeeded in freeze storage of the cells under atmospheric conditions.

In this study, we investigated the pressure tolerance of deep-sea eel cells compared to surface-dwelling organism-derived cells such as conger eel and mouse 3T3-L1 cells. To compare the pressure tolerance of each cell type, we examined (1) survival rates, (2) changes in assembly and organization of cytoskeletons, and (3) proliferation rate changes under pressure.

Materials and methods

Materials

Alexa Fluor 594 phalloidin, Alexa Fluor 488 rabbit antimouse IgG (H + L), and Live/Dead Viability/Cytotoxicity Kits were purchased from Molecular Probes Inc. (Eugene, OR, USA). Anti-tubulin (Ab-4 cocktail, clone DM1A + DM1B) was from Neo Markers (Fremont, CA, USA). Block Ace powder was from Dainippon Pharmaceutical Co., Ltd. (Osaka, Japan). Vectashield mounting medium was obtained from Vector Laboratories (Burlingame, CA, USA). The 10% formalin neutral buffer solution (pH 7.4), phosphate-buffered saline (PBS) powder, and collagenase were purchased from Wako Pure Chemical Industries (Osaka, Japan). Triton X-100 was from Sigma Chemical (T-9284, St. Louis, MO, USA). Poly-D-lysin was from Becton Dickinson Labware (Franklin Lakes, NJ, USA). Lab-Tek II chamber slides with cover (RS sterile glass slides) and 25-cm^2 culture flasks were obtained from Nalgene Nunc International (Rochester, NY, USA). Dulbecco's modified Eagle's medium (DMEM), L-15 medium, and FBS were obtained from ICN Biomedicals (Aurora, OH, USA). Trypsin/EDTA, a mixture of penicillin (5,000 IU/ml) and streptomycin (5,000 μg/ml), and a mixture of penicillin (10,000 IU/ml), streptomycin (10,000 μg/ml), and fungizone (2.5 μg/ml) were from Bio Whittaker (Walkersville, MD, USA). Dispase was from Collaborative Biomedical Products (Bedford, UK).

Cell culture

Mouse 3T3-L1 cells (Dainippon Pharmaceutical Co., Ltd.) were plated on Lab-Tek II chamber slides or in 25-cm^2 culture flasks in DMEM containing 10% (v/v) FBS and 1% (v/v) penicillin and streptomycin mixture. The cells were grown at 37°C in a humidified atmosphere of 5% CO_2 to a final density of 1–5 $\times 10^3$ cells/cm^2.

The procedures for primary culture of pectoral fin tissues from the deep-sea eel *S. parasiticus* and the epipelagic conger eel *Conger myriaster* were described elsewhere (Koyama et al. 2003a, 2003b). The pectoral fin tissue was removed using surgical scissors and transferred to artificial seawater at a temperature of 4°C containing 1% (v/v) mixture of penicillin (10,000 IU/ml), streptomycin (10,000 μg/ml), and fungizone (2.5 μg/ml) (Bio Whittaker). After a 15-min exposure, the pectoral fin tissue was rinsed twice with cold 4°C artificial seawater containing 1% the antibiotics mixture, transferred into either trypsin/EDTA 0.25 mg/ml (Bio Whittaker) or collagenase–dispase solution consisting of collagenase 0.5 mg/ml (Wako) and 10% (v/v) dispase (Collaborative Biomedical Products) in PBS containing Ca^{2+} and Mg^{2+}. Each transferred pectoral fin preparation was incubated for 20 min at 20°C. After incubation, the enzyme solutions were removed by centrifugation at 500 g for 2 min, and the minced fin tissue was resuspended in 3 ml of L-15 medium containing NaCl 4 g/l, 1% antibiotic solution consisting of penicillin (5,000 IU/ml) and streptomycin (5,000 μg/ml), and 20% (v/v) FBS. The tissue fragments were placed in 25-cm^2 tissue culture flasks. When the explant culture of fin cells ceased to spread, the minced tissues were trypsinized for 3 min at 20°C, transferred to the collagenase–dispase solution, and further incubated overnight at 4°C. The disaggregated fin cells were washed by centrifugation at 500 g for 2 min and resuspended in the L-15 medium. Following procedures, the fin cells were cultured in 25-cm^2 tissue culture flasks. Figure 1 shows the cell growth rate in conger and deep-sea eel cells under atmospheric pressure conditions. The optimal temperature for growth of conger and deep-sea eel cells was found to be 25°C and 15°C, respectively. Cell growth rates of deep-sea eel cells were extremely slow (doubling time 170 h) when thawed from liquid nitrogen temperature. The growth rates became stable after 1–2 months of cultivation. Therefore, we used the stable growth rates of the deep-

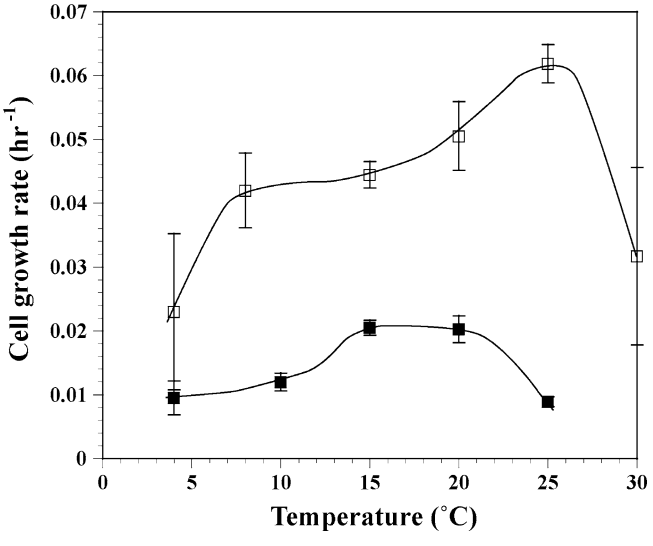

Fig. 1 Properties of conger eel and deep-sea eel cell growth under elevated temperature conditions. □ Conger eel cells, ■ deep-sea eel cells. Values were the means ± SEM (n = 8)

sea and conger eel cells that passaged from 10 to 15 times in all experiments.

Deep-sea and conger eel cells were plated on Lab-Tek II chamber slides or in 25-cm^2 culture flasks in L-15 medium containing NaCl 4 g/l, 1% antibiotic solution consisting of penicillin (5,000 IU/ml) and streptomycin (5,000 μg/ml), and 20% (v/v) FBS. The salt-enriched L-15 medium was adjusted to pH 7.3. Deep-sea and conger eel cells were grown at 15°C or 25°C in a humidified atmosphere to a final density of 1–5 $\times 10^3$ cells/cm^2 . The chamber slides were inserted into flat-bottomed glass tubes with an inside diameter of 26 mm and height of 118 mm. The cells on the chamber slides were then immersed in serum-free salt-enriched fresh L-15 medium containing the same concentrations of penicillin and streptomycin. In the case of culture flasks, the cells were immersed in serum containing fresh salt-enriched L-15 medium. After the air bubbles had been removed, the glass tubes or culture flasks were tightly sealed with parafilm (American National Can, Greenwich, CT, USA). The media volumes in the glass tubes and culture flasks were 64 and 76 ml, respectively. Thereafter, the sealed glass tubes or culture flasks were subjected to pressure.

Application of hydrostatic pressure to the cells

Cultured mouse 3T3-L1, deep-sea eel or conger eel cells at a density of 1–5 $\times$ 10^3 cells/cm^2 on Lab-Tek II chamber slides in the glass tubes or 25-cm^2 culture flasks were placed in a stainless steel pressurization vessel (Teramecs, Kyoto, Japan) connected to a hydrostatic pressure apparatus (TP200L, Teramecs). Compression and decompression rates were 3–5 MPa/s and between about −20 and −40 MPa/s, respectively. The temperature of each cell type was maintained with a water bath during pressurization. We confirmed that there were no changes in the pH of the culture medium prior to or following exposure to high hydrostatic pressure. The dissolved oxygen concentration in each medium was measured with a portable dissolved oxygen sensor (DO-21P, Toa Electronics, Tokyo, Japan) before and after pressurization, and little or no change in the dissolved oxygen concentration was detected.

Actin and tubulin staining

Cells on the chamber slides were rinsed with PBS and fixed in 10% formalin neutral buffer solution for 15 min. After fixation, the cells were washed three times in PBS for 3 min each time using a slide washer (SW-4, Juuji Field Co. Ltd., Tokyo, Japan). The cells were then replaced in 0.1% (v/v) Triton X-100 in PBS and incubated for 5 min at room temperature. Then the cells were placed in PBS and incubated for another 15 min at room temperature. The cells were further incubated in 10 g/l of Block Ace in distilled water for 60 min and washed three times with PBS for 3 min each time. For tubulin staining, the cells were reacted with anti-tubulin antibody (Ab-4 cocktail solution) for 60 min at 37°C and washed three times with PBS for 3 min each time. The cells were further reacted with a 1:200 dilution of Alexa Fluor 488 rabbit anti-mouse IgG antibody for 30 min at 37°C and washed three times with PBS for 3 min each time. For actin staining, the cells were further reacted with a 1:20 dilution of Alexa Fluor 594 phalloidin for 20 min at room temperature and washed three times with PBS for 3 min each time. After these procedures, the cells on chamber slides were mounted on Vectashield mounting medium and observed under a confocal laser scanning microscope system (Fluoview FV500 system, Olympus, Tokyo, Japan).

Cell viability test

Mouse 3T3-L1 cells were incubated with both calcein-AM 2 μM and EthD-1 4 μM (Live/Dead Viability/Cytotoxicity Kit) in PBS for 15 min at 37°C. Deep-sea and conger eel cells were incubated with both calcein-AM 2 μM and EthD-1 4 μM in PBS containing NaCl 4 g/l for 15 min at 15°C and 25°C, respectively. After incubation, cell viability was examined under a blue excitation light in accordance with the manufacturer's recommendations. Using the double-staining technique, living cells emit green fluorescence of calcein due to esterase activity. On the other hand, dead cells generate a bright red fluorescence because EthD-1 enters cells with damaged membranes. The cells were examined in random areas and were assayed by counting the percentage of living cells. More than 100 cells were counted in each test.

Measurement of doubling time

The numbers of cells attached to the growth surface were counted in eight random areas. Mouse 3T3-L1, deep-sea eel or conger eel cells were placed in 25-cm^2 culture flasks at the same cell density within the range between 1 $\times 10^3$ and 5 $\times$ 10^3 cells/cm^2 . After 1–3 days of incubation, the cells in each culture flasks were subjected to pressure for 24, 52, 72, and 100 h. The incubation temperature of mouse 3T3-L1, deep-sea eel, and conger eel cells was 37°C, 15°C, and 25°C, respectively. Doubling time was measured after 24, 52, 72, and 100 h of incubation under the pressure conditions. When no statistically significant differences in cell density between 0 and 100 h was detected, the cell growth rate was considered to be zero. Statistical analysis was performed using Student's t test. The dissolved oxygen concentration in each medium was measured using a portable dissolved oxygen sensor (DO-21P, Toa Electronics) before and after pressurization. We detected little or no change in the dissolved oxygen concentration of the medium.

Real-time observation of deep-sea eel cells under pressure

Microscopic observation of deep-sea eel cells was performed using a pressure chamber system equipped with high-pressure pumps to perfuse the chamber with culture medium continuously to provide nutrition and oxygen to the cells under pressures ranging from atmospheric pressure to 100 MPa (Koyama et al. 2001).

A 2-mm-thick cover glass was coated with poly-D-lysine 0.1 mg/ml in PBS for 1 h at 37°C. Thereafter, the cover glass was washed with PBS. The deep-sea eel cells were seeded on the cover glass and cultured in salt-enriched L-15 medium supplemented with 20% (v/v) FBS, penicillin 50 IU/ml, and streptomycin 50 μg/ml. The cells were grown to a cell density of 30–70 cells/3.14 mm^2 over 3–7 days at 15°C in a humidified atmosphere. The cover glass was placed in the pressure chamber system that was filled with salt-enriched L-15 medium. The perfusion medium was adjusted to pH 7.3. The cells were then exposed to hydrostatic pressure. The median perfusion speed was set at 6 μl/h.

Results

Survival rates of deep-sea eel, conger eel, and mouse 3T3-L1 cells under pressure

Survival rates of deep-sea eel, conger eel, and mouse 3T3-L1 cells were examined after exposure to high hydrostatic pressure. Each cell type was grown to 1–5 × 10^3 cells/cm^2 under atmospheric pressure conditions and then exposed to hydrostatic pressure varying from 5 to 200 MPa (0.1 MPa = 1 bar) for 20 min. After pressurization, cell viability was investigated using double staining with both calcein-AM and EthD-1 as described in "Materials and methods." More than 100 cells were assayed by counting the percentage of living cells. Figure 2 shows the survival rates of mouse 3T3-L1, conger eel cells, and deep-sea eel cells after pressurization. The majority (>95%) of mouse 3T3-L1 cells remained alive at pressure up to 60 MPa (Fig. 2). At pressure of 70 MPa, more than 70% of mouse 3T3-L1 cells were damaged or died based on the bright red fluorescence of EthD-1 (Fig. 2). No living mouse 3T3-L1 cells were found on the Lab-TeK II chamber slides at 100 MPa (Fig. 2). Conger eel cells at 25°C remained alive at pressure up to 60 MPa (Fig. 2). All of the conger eel cells were damaged or died at 130 MPa (Fig. 2). Conger eel cells at 15°C began to sustain damage or die at pressure of only 5 MPa (Fig. 2). Although no living mouse and conger eel cells were found at the pressure of 130 MPa, all deep-sea eel cells remained alive on the chamber slides until the pressure reached 150 MPa (Fig. 2). All of the living deep-sea eel cells detached from the growth surface of the chamber slide at 175 MPa. At 200 MPa, all deep-sea eel cells collapsed and died (Fig. 2). The deep-sea eel cells thus survived at higher pressure than did the mouse and conger eel cells. In the subsequent three experiments, temperature conditions for deep-sea eel, conger eel, and mouse 3T3-L1 cells were set at the growth optima of 15°C, 25°C, and 37°C, respectively.

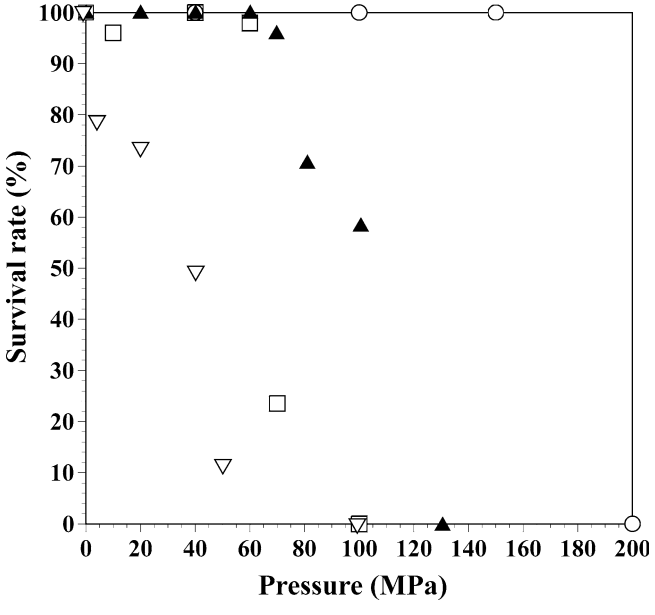

Fig. 2 Survival rates of mouse 3T3-L1, conger eel, and deep-sea eel cells under elevated pressure conditions. ○ Deep-sea eel cells at 15°C, ▲ conger eel cells at 25°C, □ mouse 3T3-L1 cells at 37°C, ▽ conger eel cells at 15°C. Each cell type was grown to 1–5 × 10^3 cells/cm^2 and subjected to pressure ranging from 5 to 200 MPa for 20 min. After pressurization, the viability of more than 100 cells was investigated using the calcein-AM and EthD-1 double-staining method

Changes in assembly and organization of cytoskeletons under pressure

We examined the depolymerization of actin and tubulin filaments after the application of hydrostatic pressure and compared the results among deep-sea eel, conger eel, and mouse 3T3-L1 cells (Figs. 3, 4). Each cell type was grown to 1–5 × 10^3 cells/cm^2 and then exposed to hydrostatic pressure varying from 40 to 130 MPa for 20 min. After pressurization, the change in the distribution of actin and tubulin in the cells was examined. Figures 3 and 4 show fluorescent immunostaining of actin and tubulin filaments in the three cell types. In mouse 3T3-L1 and conger eel cells, hydrostatic pressure of 40 MPa induced disruption of the cytoskeletal organization with profound changes in cell shape (Fig. 3e–h). Meanwhile, little change in cell shape with depolymerization of actin and tubulin filaments was observed in deep-sea eel cells at hydrostatic pressure of 40 MPa (Fig. 4b, f). We observed that most microtubules and some actin filaments in deep-sea eel cells began to be disrupted at 100 MPa (Fig. 4c, g). At 130 MPa, all of the microtubules and a majority of the actin filaments depolymerized in the deep-sea eel cells

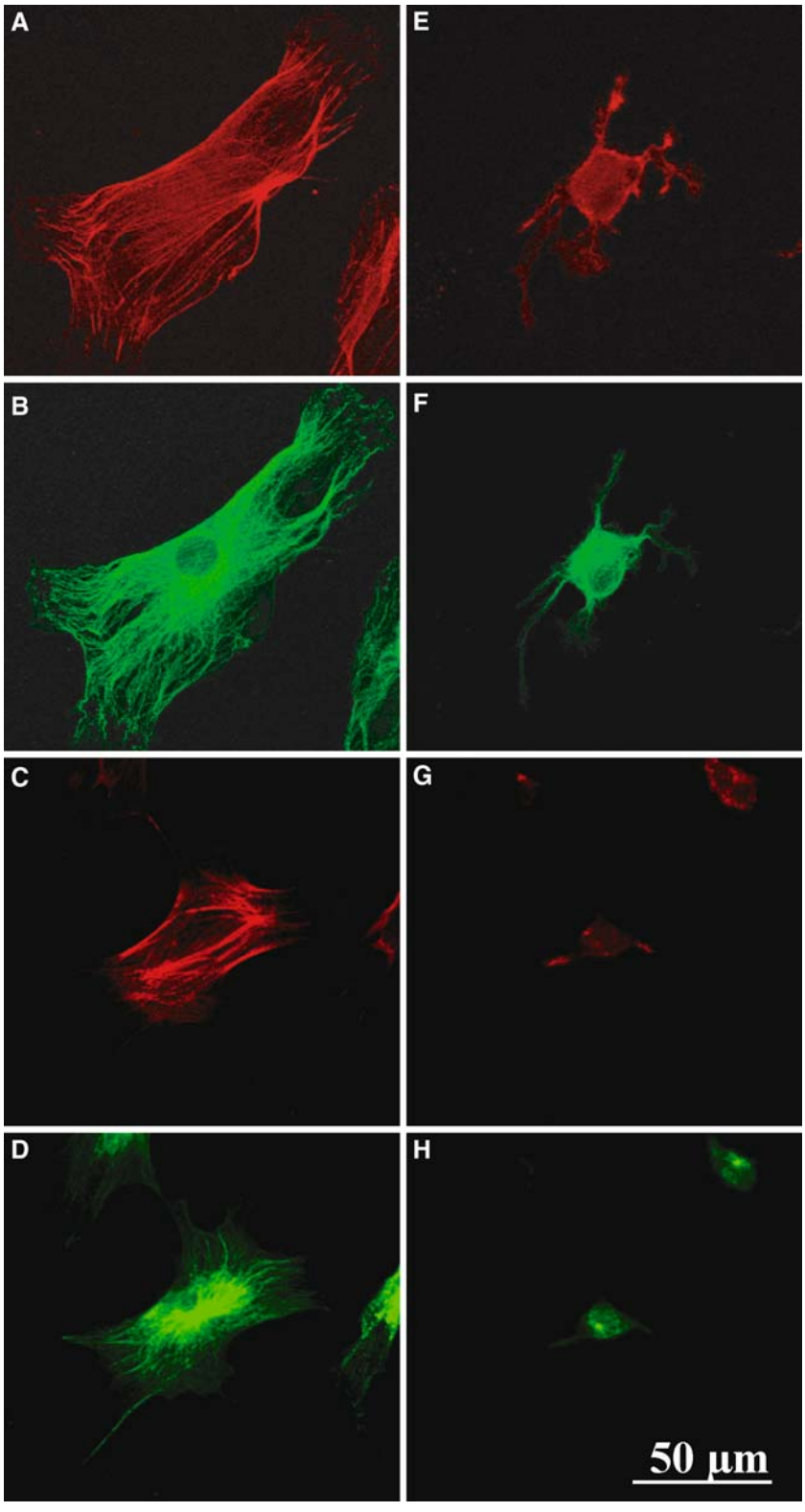

Fig. 3 Pressure-induced actin and tubulin depolymerization in mouse 3T3-L1 and conger eel cells. Each cell type was grown to $1–5 \times 10^3$ cells/cm^2 and subjected to pressure of 40 MPa for 20 min. The temperature of the conger eel and mouse 3T3-L1 cells was set at the growth optima of 25°C and 37°C, respectively. *Red and green fluorescence* indicates actin and tubulin filaments, respectively. **a–d**Under atmospheric conditions. **e–h** After pressurization. **a, b, e, f** Mouse 3T3-L1 cells. **c, d, g, h** Conger eel cells

(Fig. 4d, h). A part of the deep-sea eel cells induced profound cell-shape changes (10–20% of total cells) by pressure application between 60 and 130 MPa for 20 min.

Recovery of pressure-induced cell-shape changes

We investigated the recovery process from pressure-induced profound morphologic changes in 3T3-L1, conger

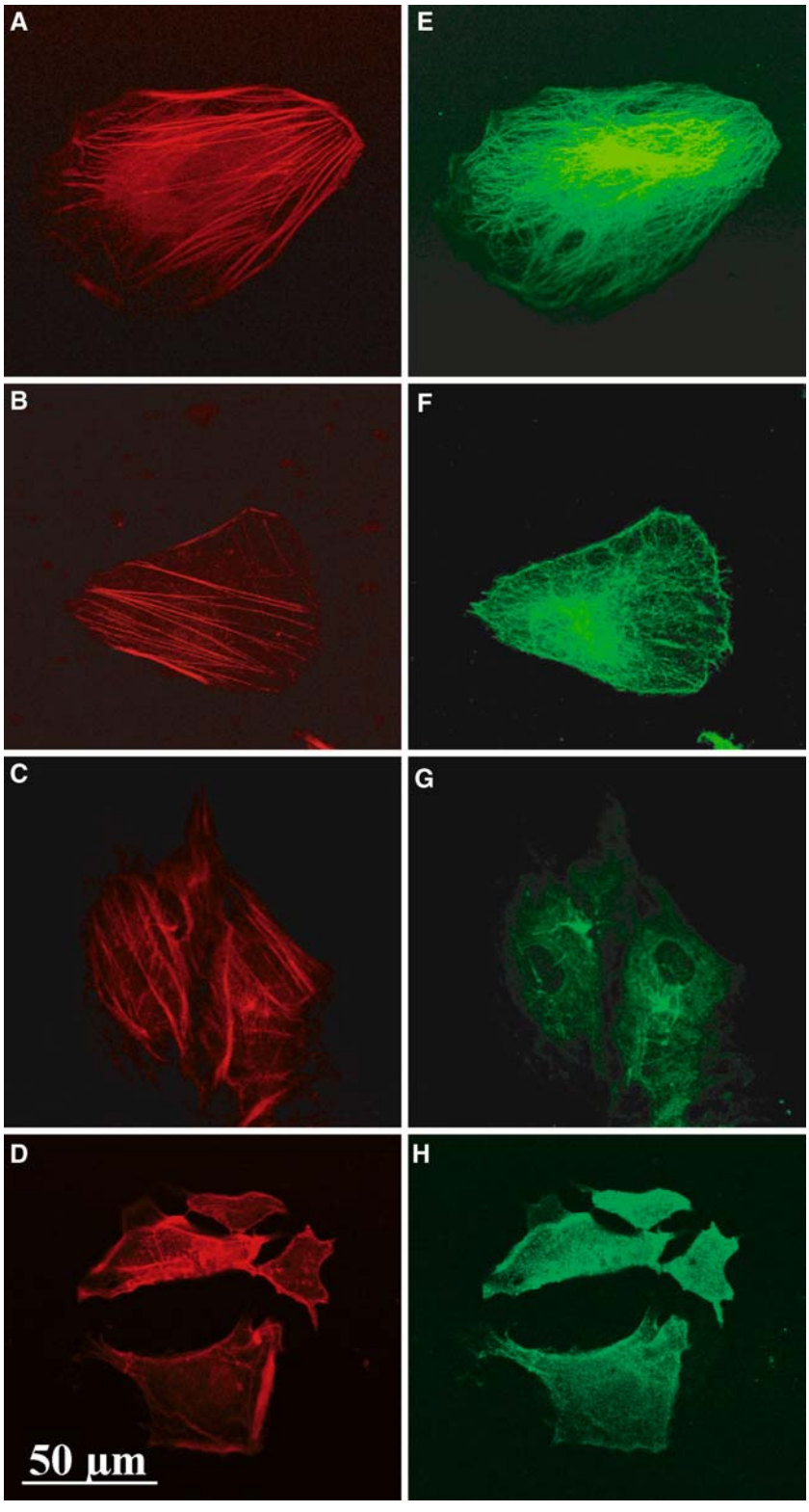

Fig. 4 Actin and tubulin filaments in deep-sea eel cells at high pressure. Deep-sea eel cells were grown to 1–5 × 10^3 cells/cm^2 and subjected to pressure ranging from 40 to 130 MPa for 20 min at 15°C. *Red and green fluorescence* indicate actin and tubulin filaments, respectively. **a, e** Atmospheric conditions. **b, f** At 40 MPa. **c, g** At 100 MPa. **d, h** At 130 MPa

eel, and deep-sea eel cells (Fig. 5). In mammalian cells, pressure-induced morphologic changes with disruption of the cytoskeletal organization were reversible until reaching the pressure of 60 MPa for 20 min (Landau 1960, 1961). After pressure release, the mammalian cells respread filopodia and grew normally through the cell cycle (Landau 1960, 1961). Mouse 3T3-L1 and conger eel cells also showed the same phenomena and the pressure-induced profound cell-shape changes were reversible and normally through the cell cycle until

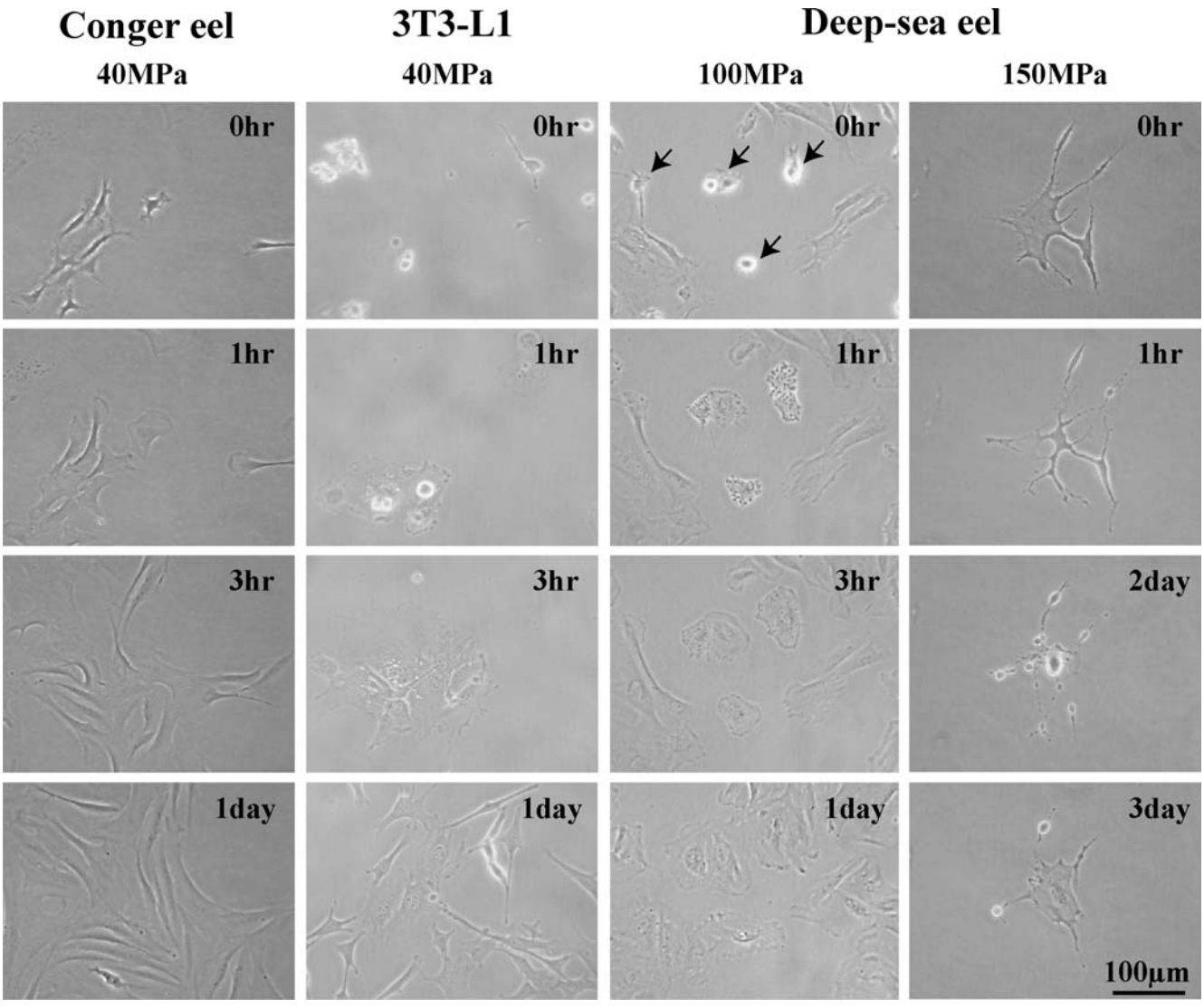

Fig. 5 Recovery processes from pressure-induced morphologic changes. Conger eel, mouse 3T3-L1, and deep-sea eel cells were grown to 1–5 × 10^3 cells/cm^2 and subjected to pressure of 40, 100, or 150 MPa for 20 min. After pressurization, cell recovery processes were observed after the cultivation under atmospheric conditions. The temperature of the conger eel, mouse 3T3-L1, and deep-sea eel cells was set at the growth optima of 25°C, 37°C, and 15°C. *The arrows* indicated pressure-induced profound morphological change in the deep-sea eel cells

60 MPa (Fig. 5). In deep-sea eel, a part of the cells (10–20% of total cells) induced profound cell-shape changes such as cell rounding (Fig. 5 *indicated by arrows*) after the pressure application between 60 and 130 MPa for 20 min. At 150 MPa for 20 min, the ratio of the pressure-induced cell rounding increased about 40% of the total deep-sea eel cells. The pressure-induced morphologic changes were reversible until pressure of 100 MPa for 20 min (Fig. 5). The cells recovered from morphologic change after 3 h and grew normally after 1 day of cultivation (Fig. 5). At pressure of 150 MPa, the deep-sea eel cells exhibited delayed recovery from morphologic change but were repaired after 3–4 days of cultivation (Fig. 5). Although deep-sea eel cells recovered their shape, the cells at pressures of 125 MPa and greater did not grow. Therefore, we investigated the distribution patterns of actin and tubulin filaments in the pressurized deep-sea eel cells.

Figure 6 shows fluorescent staining of actin and tubulin filaments in the deep-sea eel cells after recovery from pressure-induced morphologic change. At the pressure of 100 MPa, the cells showed repair of actin and tubulin filament structures after 1 h of incubation (Fig. 6). After application of pressure of 125 and 150 MPa, microtubule structures in the deep-sea eel cells were not repaired during 1 month of incubation, although the actin filament structure recovered after pressure release (Fig. 6). The results in Fig. 6 indicate that the inactivation of tubulin polymerization is one of the reasons that causes pressure-induced inhibition of deep-sea eel cell growth.

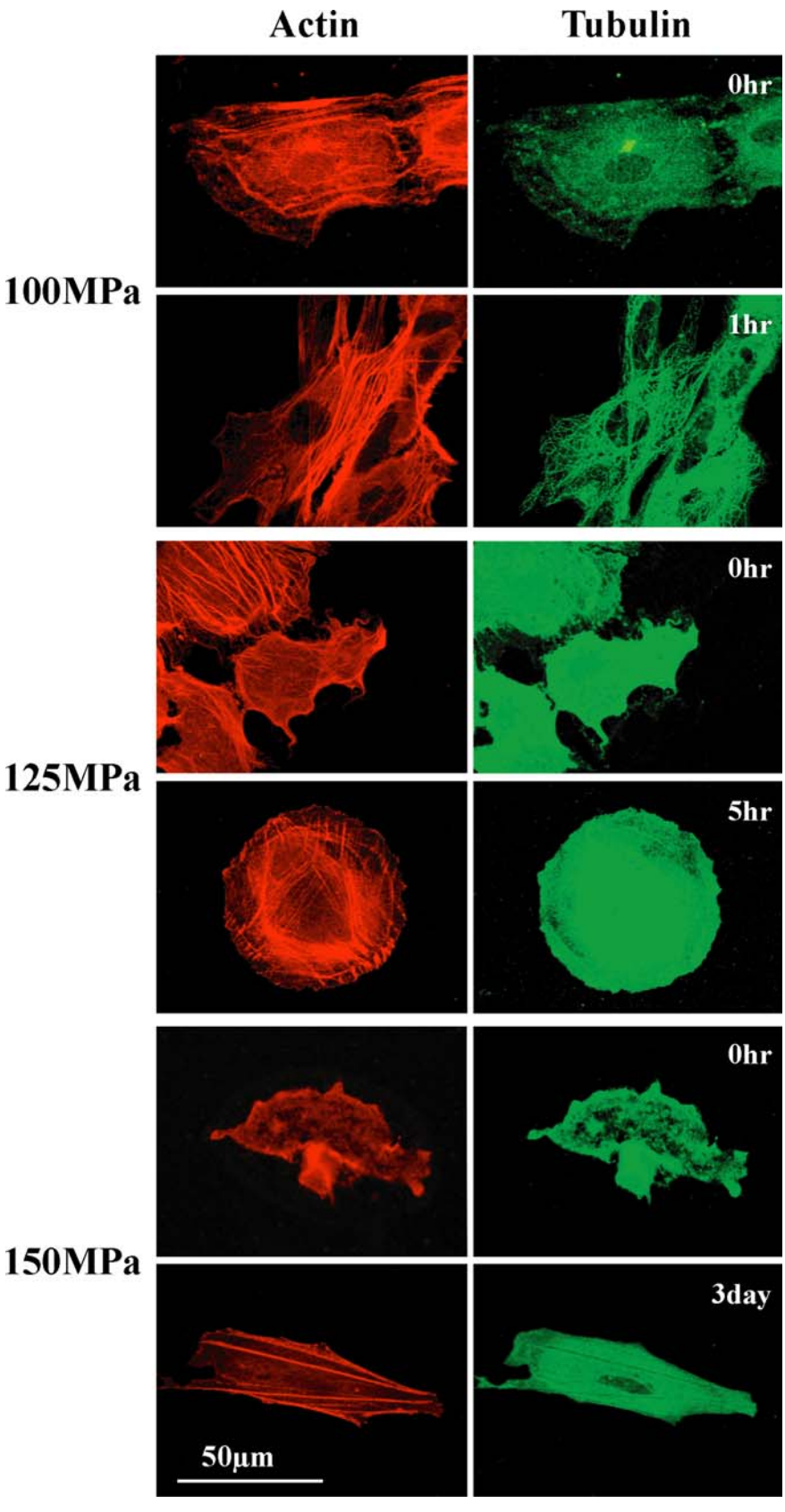

Fig. 6 Recovery processes of pressure-induced cytoskeletal disorganization in deep-sea eel cells. Deep-sea eel cells were grown to $1–5 \times 10^3$ cells/cm^2 and subjected to pressure ranging from 100 to 150 MPa for 20 min at 15°C. After pressurization, the cell recovery processes of actin and tubulin filaments were observed

Cell proliferation of mouse 3T3-L1, conger eel, and deep-sea eel cells under pressure

We examined the cell proliferation rates of deep-sea eel, conger eel, and mouse 3T3-L1 cells under pressure (Fig. 7). Each cell type was placed in 25-cm^2 culture flasks at a density of 1–5 $\times$ 10^3 cells/cm^2 . The numbers of cells attached to the growth surface were counted in eight random areas (each 1 mm^2) after 0, 24, 52, 72, and 100 h of incubation under the respective pressure conditions. When no statistically significant differences in cell density between 0 and 100 h was detected, the cell growth rate was considered to be zero. The results in Fig. 7 show that conger eel cells were sensitive to high hydrostatic pressure and did not grow at 10 MPa. Mouse 3T3-L1 cells on the other hand grew more rapidly under the pressure of 5 MPa than at atmospheric pressure and stopped growing at 18 MPa (Fig. 7). Although surface-dwelling organism-derived cells such as mouse and conger eel cells did not grow at pressure greater than 18 MPa, deep-sea eel cells were capable of growth up to high hydrostatic pressure of 25 MPa (Fig. 7). Cell growth rate of the deep-sea eel cells were of no statistical differences between 20 MPa pressure and atmospheric conditions (Fig. 7).

To investigate the M phase of deep-sea eel cells under pressure, we observed the cell division process using an optical pressure chamber system (Koyama et al. 2001). Figure 8 shows real-time observation of deep-sea eel cells under pressure. Most animal cells, including deep-sea eel cells, reaching the M phase, in which nuclear and cytoplasmic divisions occur, requires 1 h at atmospheric pressure (Koyama et al. 2003a, 2003b). In this experiment, the period between beginning of cell rounding and end of cell division considered to be M phase. Based on our microscopic observations, deep-sea eel cells require 4 h to reach the M phase under pressure of 20 MPa (Fig. 8). At the pressure of 30 MPa, the morphology of deep-sea eel cells began to change after 2 days of cultivation (Fig. 8).

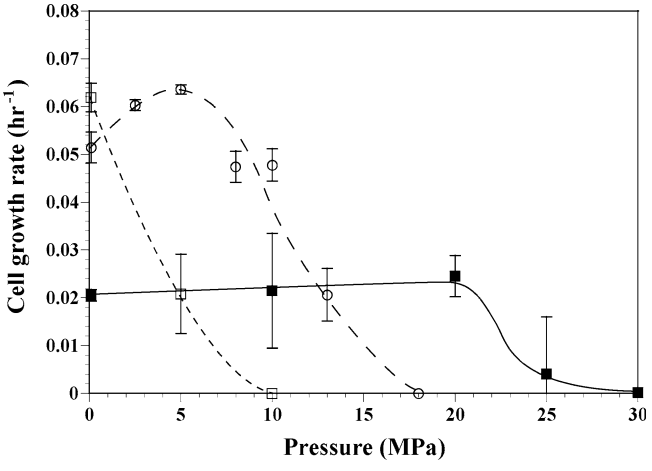

Fig. 7 Properties of cell growth under elevated hydrostatic pressure conditions. Mouse 3T3-L1 (○), deep-sea eel (■), or conger eel cells (□) were placed in 25-cm^2 culture flasks at the same cell density within the ranges between 1 $\times$10^3 and 5 $\times$ 10^3 cells/cm^2 . The cells in each culture flask were subjected to pressure for 24, 52, 72, and 100 h, respectively. The incubation temperature of mouse 3T3-L1, deep-sea eel, and conger eel cells were 37°C, 15°C, and 25°C, respectively. When no statistically significant differences in cell density between 0 and 100 h was detected, the cell growth rate was considered to be zero. Values were the means ± SEM (n = 8)

Discussion

In this study, we demonstrated that the deep-sea eel-derived cells had greater pressure tolerance than conger eel and mouse 3T3-L1 cells. This conclusion is supported by the survival rate results (Fig. 2), cytoskeletal disorganization (Figs. 3, 4), recovery from the cell-shape changes (Figs. 5, 6), and cell proliferation rates under pressure (Figs. 7, 8). Although no living mouse and conger eel cells were found at pressures of 100 and 130 MPa, the deep-sea eel cells remained alive when subjected to pressure of less than 150 MPa for 20 min (Fig. 2). The cell viability test was performed using calcein-AM and EthD-1 double staining. Using this technique, dead cells emit red fluorescence due to the EthD-1 that enters cells with damaged membranes. Pressure decreases membrane fluidity by compressing the bilayer laterally because the surface area per phospholipid molecule decreases, closer packing of acyl chains results in reduced molecular mobility, and an increase in van der Waals interactions occurs (Stamatoff et al. 1978; Braganza and Worcester 1986; reviewed in Gibbs 1997). Differences in membrane lipid composition and membrane fluidity might affect the survival rates of each cell type (Fig. 2). This hypothesis is supported by the facts that species from greater depths have a greater proportion of unsaturated fatty acids in mitochondrial membranes (Cossins and Macdonald 1986), and brain myelin membranes are more fluid in deep-sea fish than in shallow-living species (Cossins and Macdonald 1984; Behan et al. 1992; reviewed in Gibbs 1997).

In mammalian tissue cells, hydrostatic pressure of 30–60 MPa for 20 min reversibly induces morphologic changes accompanied by cytoskeletal depolymerization (Landau 1960, 1961; Bourns et al. 1988; Crenshaw et al. 1996). After pressure is released, the cells respread and progress normally through the cell cycle (Landau 1960, 1961). In contrast, the deep-sea eel cells reversibly underwent actin and tubulin depolymerization when subjected to hydrostatic pressure of 100 MPa (Fig. 6). Increased hydrostatic pressure shifted the self-assembly equilibrium of cytoskeletal proteins toward depolymerization, and promoted the disassembly of actin (Swezey and Somero 1985; Morita 2003), myosin II (Davis 1981, 1985), and tubulin (Salmon 1975). The cytoskeletons from surface-dwelling organisms are much more pressure sensitive because polymerization of these proteins in vitro entails large increases in volume (~100 ml/mol). In deep-sea species, the association constant for

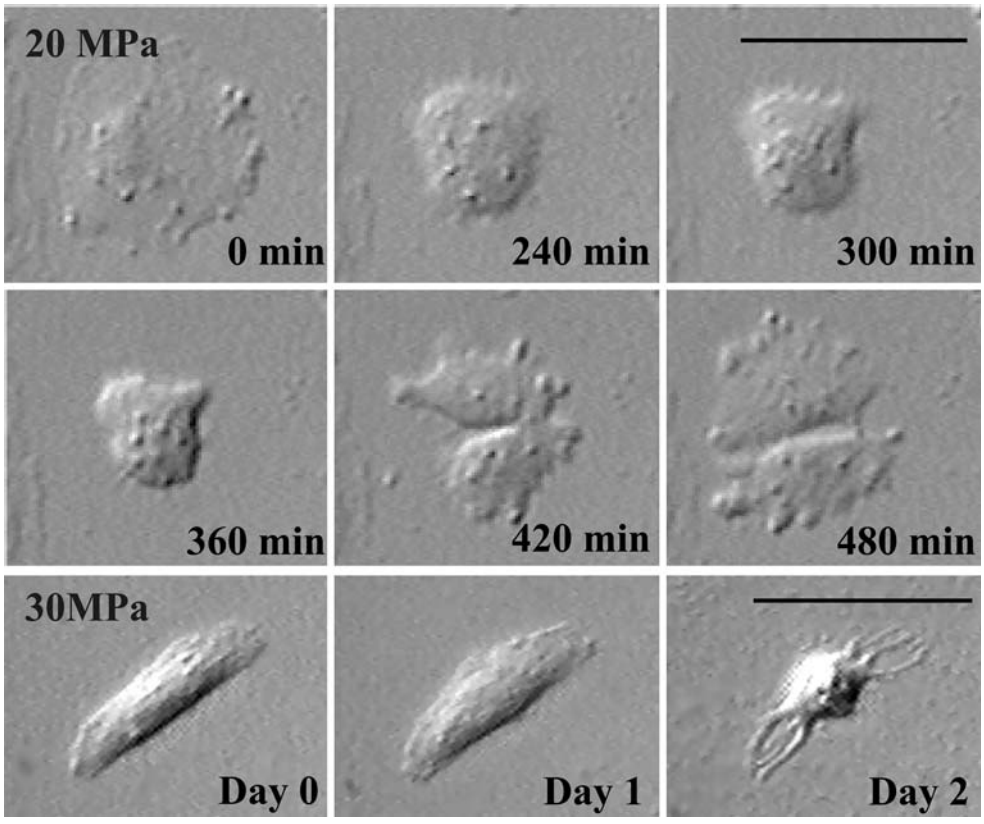

Fig. 8 Real-time observation of cultured deep-sea eel cells under pressure. A 2-mm-thick cover glass was coated with poly-D-lysine 0.1 mg/ml in PBS for 1 h at 37°C and then washed with PBS. Deep-sea eel cells were seeded on a 2-mm-thick cover glass coated with poly-D-lysine and grown to a cell density of 30–70 cells/3.14 mm^2 for 3–7 days at 15°C in a humidified atmosphere. The cells on the cover glass were placed in the optical pressure chamber system (Koyama et al. 2001) and exposed to hydrostatic pressure. The median perfusion speed was set at 6 µl/h. *Bars* indicate 50 µm

polymerization of actin from *Coryphaenoides armatus* and *Coryphaenoides yaquinae*, rattail fish occurring at depths of 2,700–5,000 m (pressure 27–51 MPa) and 4,000–6,400 m (pressure 41–65 MPa), respectively, are relatively unaffected by pressure, with a small volume change associated with polymerization of less than 20 ml/mol (Swezey and Somero 1985; Morita 2003). From amino acid sequence analysis of actin species, only three substitutions—V54A or L67P, Q137K, and A155S—distinguish abyssal and nonabyssal actins from *Coryphaenoides* sp. (Morita 2003). Our results in Figs. 3 and 4 appear to indicate that a few amino acid substitutions in key functional positions of cytoskeletal proteins reduce the volume change associated with cytoskeletal polymerization and thereby alter the pressure sensitivity of the cell-shape changes.

Although the deep-sea eel cells remained alive at the pressure of 150 MPa for 20 min (Fig. 2), they did not grow under pressure of 30 MPa (Figs. 7, 8). Moreover, the deep-sea eel cell morphology changed after 2 days of cultivation at pressure of 30 MPa (Fig. 8). When subjected to pressure of 20 MPa, deep-sea eel cells required 4 h to finish the M phase (Fig. 8), which is longer than required under atmospheric conditions. Hydrostatic pressure of 30 MPa for 2 days might inhibit mitochondrial activities in deep-sea eel cells. In addition to altering the thermodynamics of the assembly of cytoskeletal proteins (Heremans 1982; Crenshaw et al. 1996; Mozhaev et al. 1996), decreases in ATP and GTP levels due to mitochondrial inactivation would also be involved in the morphologic changes in deep-sea eel cells concomitant with actin and tubulin depolymerization.

In lactate dehydrogenase studies of the deep-sea fish *Sebastolobus altivelis*, hydrostatic pressure of greater than 6.8 MPa increased the Michaelis constant (K_m) of NADH by threefold and inhibited maximal activities (V_{max}) at 34 MPa by 11% (Siebenaller and Somero 1979; reviewed in Gibbs 1997). The deep-sea fish *S. altivelis* commonly occur at depths between 550 and 1,300 m (habitat pressure, 5.6–13 MPa) (Siebenaller and Somero 1979). Our deep-sea eel cells were from the pectoral fin tissues of *S. parasiticus* that inhabits depths between 366 and 2,630 m (habitat pressure, 3.7–27 MPa) (Nakabo 2000). The expression of some intracellular proteins in deep-sea eel cells might be inhibited under hydrostatic pressure conditions of 30 MPa and greater.

Application of 125 MPa and over hydrostatic pressure induced inactivation of tubulin polymerization (Fig. 6). The deep-sea eel cells did not proliferate during 1 month, in as much as the microtubule structures were not repaired. Decreasing intracellular GTP contents and/or the pressure-induced microtubule structural deficiency might cause the inactivation of the tubulin polymerization because the actin filament structure recovered after pressure release (Fig. 6) and the deep-sea eel cells kept alive (Fig. 2).

In the results shown in Fig. 7, the cell proliferation rate of mouse 3T3-L1 cells increased by 27% at 5 MPa compared with the rate under atmospheric conditions.

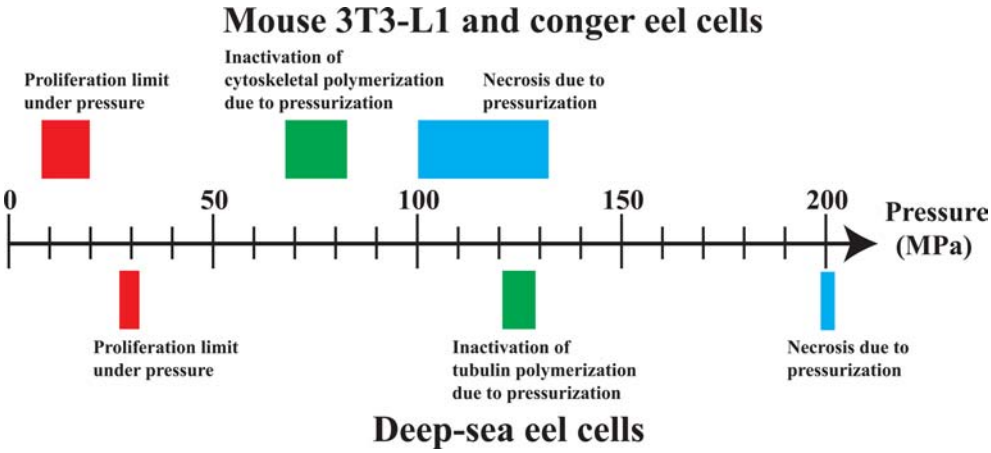

Fig. 9 Schematic illustration of cumulative pressure-induced effects on mouse 3T3-L1, conger eel, and deep-sea eel cells

Several researchers reported that the application of weak pressure, such as gas pressure of 4–12 kPa and H_2O pressure of 0.4 kPa, stimulated cell proliferation of rat mesangial cells and human umbilical vein endothelial cells, respectively (Kawata et al. 1998; Schwartz et al. 1999).

What remains unclear is why does it take the deep-sea eel cells so long to reach M phase in the optical pressure chamber at 20 MPa (Fig. 8). Cell growth rate of the deep-sea eel cells is not so different between 0.1 and 20 MPa in Fig. 7. M phase needs a lot of chemical reactions that accompanies with ATP consumptions (Alberts et al. 2002). Hydrostatic pressure would increase K_m and decrease V_{max} of enzyme reactions (Siebenaller and Somero 1979; reviewed in Gibbs 1997); therefore, M phase under pressure might need more times compared to the atmospheric condition. Same as M phase, S phase would also be needed more times compared with G1 and G2 phases because S phase also required lots of chemical reactions with ATP consumptions (Alberts et al. 2002).

Hydrostatic pressure-induced cytokine gene expression and secretion involve PKC activation in normal human dermal fibroblasts (Koyama et al. 2002b; Koyama and Aizawa 2002). Because some cell types can be stimulated to proliferate in culture when PKC is activated (Alberts et al. 2002), the mechanisms of pressure-stimulated cell proliferation in mouse 3T3-L1 cells might involve activation of PKC-signaling cascades. Our cumulative results in this study are summarized in Fig. 9.

Acknowledgements This study was supported by Grant-in-Aid for Young Scientist (A) (No. 14704007) and Grant-in-Aid for Exploratory Research (No. 15656214) from the Ministry of Education, Culture, Sports, Science and Technology of Japan.

References

Alberts B, Johnson A, Lewis J, Raff M, Roberts K, Walter P (2002) Molecular biology of the cell, 4th edn. Garland Science, New York

Behan MK, Macdonald AG, Jones GR, Cossins AR (1992) Homeoviscous adaptation under pressure: the pressure dependence of membrane order in brain myelin membranes of deep-sea fish. Biochim Biophys Acta 1103:317–323

Bourns B, Franklin S, Cassimeris L, Salmon ED (1988) High hydrostatic pressure effects in vivo: changes in cell morphology, microtubule assembly, and actin organization. Cell Motil Cytoskeleton 10:380–390

Braganza LF, Worcester DL (1986) Structural changes in lipid bilayers and biological membranes caused by hydrostatic pressure. Biochemistry 25:7484–7488

Cossins AR, Macdonald AG (1984) Homeoviscous theory under pressure II. The molecular order of membranes from deep-sea fish. Biochim Biophys Acta 776:144–150

Cossins AR, Macdonald AG (1986) Homeoviscous adaptation under pressure. III. The fatty acid composition of liver mitochondrial phospholipids of deep-sea fish. Biochim Biophys Acta 860:325–335

Crenshaw HC, Allen JA, Skeen V, Harris A, Salmon ED (1996) Hydrostatic pressure has different effects on the assembly of tubulin, actin, myosin II, vinculin, talin, vimentin, and cytokeratin in mammalian tissue cells. Exp Cell Res 227:285–297

Davis JS (1981) Pressure-jump studies on the length-regulation kinetics of the self-assembly of myosin from vertebrate skeletal muscle into thick filament. Biochem J 197:309–314

Davis JS (1985) Kinetics and thermodynamics of the assembly of the parallel- and antiparallel-packed sections of synthetic thick filaments of skeletal myosin: a pressure-jump study. Biochemistry 24:5263–5269

Gibbs AG (1997) Biochemistry at depth. In: Randall DJ, Farrell AP (eds) Deep-sea fishes. Academic, San Diego, pp 239–277

Heremans K (1982) High pressure effects on proteins and other biomolecules. Annu Rev Biophys Bioeng 11:1–21

Kawata Y, Fujii Z, Sakumura T, Kitano M, Suzuki N, Matsuzaki M (1998) High pressure conditions promote the proliferation of rat cultured mesangial cells. Biochim Biophys Acta 1401:195–202

Koyama S, Aizawa M (2000) Tissue culture of the deep-sea bivalve *Calyptogena soyoae*. Extremophiles 4:385–389

Koyama S, Aizawa M (2002) PKC-dependent IL-6 production and inhibition of IL-8 production by PKC activation in normal human skin fibroblasts under extremely high hydrostatic pressure. Extremophiles 6:413–418

Koyama S, Miwa T, Sato T, Aizawa M (2001) Optical chamber system designed for microscopic observation of living cells under extremely high hydrostatic pressure. Extremophiles 5:409–415

Koyama S, Miwa T, Horii M, Ishikawa Y, Horikoshi K, Aizawa M (2002a) Pressure-stat aquarium system designed for capturing and maintaining deep-sea organisms. Deep-Sea Res I 49:2095–2102

Koyama S, Fujii S, Aizawa M (2002b) Post-transcriptional regulation of immunomodulatory cytokines production in human skin fibroblasts by intense mechanical stresses. J Biosci Bioeng 93:234–239

Koyama S, Horii M, Miwa T, Aizawa M (2003a) Tissue culture of the deep-sea eel *Simenchelys parasiticus* collected at 1,162 m. Extremophiles 7:245–248

Koyama S, Horii M, Miwa T, Aizawa M (2003b) Erratum. Extremophiles 7:340

Koyama S, Nagahama T, Ootsu N, Takayama T, Horii M, Konishi S, Miwa T, Ishikawa Y, Aizawa M (2005) Survival of deep-sea shrimp (*Alvinocaris* sp.) during decompression and larval hatching at atmospheric pressure. Marine Biotechnol. DOI 10.1007/s10126-004-3050-0

Landau JV (1960) Sol–gel transformations in fibroblasts of embryonic chick heart tissue: a pressure–temperature study. Exp Cell Res 21:78–87

Landau JV (1961) The effects of high hydrostatic pressure on human cells in primary and continuous culture. Exp Cell Res 23:538–548

Morita T (2003) Structure-based analysis of high pressure adaptation of α-actin. J Biol Chem 278:28060–28066

Mozhaev VV, Heremans K, Frank J, Masson P, Balny C (1986) High pressure effects on protein structure and function. Proteins 24:81–91

Nakabo T (2000) Fishes of Japan with pictorial keys to the species, 2nd edn. Tokai University Press, Tokyo

Salmon ED (1975) Pressure-induced depolymerization of brain microtubules in vitro. Science 189:884–886

Schwartz EA, Bizios R, Medow MS, Gerritsen ME (1999) Exposure of human vascular endothelial cells to sustained hydrostatic pressure stimulates proliferation: involvement of the αv integrins. Circ Res 84:315–322

Siebenaller JF, Somero GN (1979) Pressure-adaptive differences in the binding and catalytic properties of muscle-type (M4) lactate dehydrogenases of shallow- and deep-living marine fishes. J Comp Phys B 129:295–300

Stamatoff J, Guillon D, Powers L, Cladis P, Aadsen D (1978) X-ray diffraction measurements of dipalmitoylphosphatidylcholine as a function of pressure. Biochem Biophys Res Commun 85:724–728

Swezey R, Somero GN (1985) Pressure effects on actin self-assembly: interspecific differences in the equilibrium and kinetics of the G and F transformation. Biochemistry 24:852–860